PHYSICAL EXCHANGES AT THE AIR–SEA INTERFACE

UK–SOLAS Field Measurements

BY IAN M. BROOKS, MARGARET J. YELLAND, ROBERT C. UPSTILL-GODDARD, PHILIP D. NIGHTINGALE, STEVE ARCHER, ERIC D'ASARO, RACHAEL BEALE, CORY BEATTY, BYRON BLOMQUIST, A. ANTHONY BLOOM, BARBARA J. BROOKS, JOHN CLUDERAY, DAVID COLES, JOHN DACEY, MICHAEL DEGRANDPRE, JO DIXON, WILLIAM M. DRENNAN, JOSEPH GABRIELE, LAURA GOLDSON, NICK HARDMAN-MOUNTFORD, MARTIN K. HILL, MATT HORN, PING-CHANG HSUEH, BARRY HUEBERT, GERRIT DE LEEUW, TIMOTHY G. LEIGHTON, MALCOLM LIDDICOAT, JUSTIN J. N. LINGARD, CRAIG MCNEIL, JAMES B. MCQUAID, BEN I. MOAT, GERALD MOORE, CRAIG NEILL, SARAH J. NORRIS, SIMON O'DOHERTY, ROBIN W. PASCAL, JOHN PRYTHERCH, MIKE REBOZO, ERIK SAHLEE, MATT SALTER, UTE SCHUSTER, INGUNN SKJELVAN, HANS SLAGTER, MICHAEL H. SMITH, PAUL D. SMITH, MERIC SROKOSZ, JOHN A. STEPHENS, PETER K. TAYLOR, MACIEJ TELSZEWSKI, ROISIN WALSH, BRIAN WARD, DAVID K. WOOLF, DICKON YOUNG, AND HENK ZEMMELINK

A series of research cruises bring a wide array of techniques to bear on the problem of parameterizing processes that influence aerosol production and the atmospheric content of radiatively important gases, including CO_2.

The Surface Ocean–Lower Atmosphere Study (SOLAS) is an international program with the goal of achieving a "quantitative understanding of the key biogeochemical–physical interactions and feedbacks between the ocean and the atmosphere, and of how this coupled system affects and is affected by climate and environmental change" (Liss et al. 2003). A major focus of SOLAS is to understand the physical exchange processes at the air–sea interface, and in particular their influence on the flux of CO_2 and other radiatively important gases—such as CH_4, N_2O, and dimethylsulfide (DMS)—and on the production of sea spray aerosol. As part of the U.K. contribution to SOLAS, several related projects undertook field studies of the exchange processes: the Deep Ocean Gas Exchange Experiment (DOGEE), the Sea Spray, Gas Flux and Whitecap (SEASAW) study, and High Wind Air–Sea Exchanges (HiWASE). Adopting complementary approaches to the study of surface exchange processes, and sharing both some ship time and participants, they form a coherent strand of the UK–SOLAS program.

BACKGROUND. Gas exchange across the air–sea interface is an important, sometimes dominant, term in many biogeochemical cycles; it exerts a significant control on atmospheric composition and thus on climate change. The rate of gas exchange as a function of environmental conditions remains a major source of uncertainty; the gas flux is a product of the concentration difference between atmosphere and ocean and a gas transfer velocity k_w, which is dependent on the complex interactions controlling interfacial turbulence (Jähne et al. 1987). Parameterizations of k_w remain inadequate—most are formulated as simple functions of the mean wind

speed U, although some studies have shown stronger correlation with other factors, such as the mean square slope of wind-driven waves (Bock et al. 1999) and fractional whitecap coverage (Asher et al. 1995). The commonly accepted range for the dependency of k_w on U for CO_2 varies between roughly U^2 and U^3 (e.g., Liss and Merlivat 1986; Wanninkhof 1992; Wanninkhof and McGillis 1999; Nightingale et al. 2000; Wanninkhof et al. 2004). The transfer velocity for different gases, however, depends strongly on solubility, and measurements of k_w for DMS, for example, show it to vary much less strongly with wind speed (Huebert et al. 2004). The divergence of the parameterizations for k_w at high wind speeds presents a serious issue as a result of the disproportionately large influence of very high winds on the mean flux. The use of different parameterizations within different climate models results in a wide variety of long-term forecasts, contributing considerable uncertainty in assessing future climate (McGillis et al. 2001).

The uncertainty in the behavior of k_w results in part from a paucity of measurements—to date only a small number of studies have made direct gas flux measurements over the oceans, and very few have observed winds above 15 m s^{-1}—and in the disparity between the short time scales on which the controlling processes operate and the typically much longer averaging time for measurements such as deliberate tracer release experiments (Asher et al. 2004). Although the dependence on wind speed is strong, it cannot account for all the variability observed in k_w. Other factors believed to exert a controlling influence include atmospheric stability, sea state, wave breaking, whitecapping and bubble bursting, sea surface temperature, rain, wind stress, and the presence of surfactants and organics (e.g., Woolf 1997, 2005; Ho et al. 2000; Frew et al. 2004). None of this complexity is represented in most parameterization schemes, although the National Oceanic and Atmospheric Administration (NOAA)–Coupled Ocean–Atmosphere Response Experiment (COARE) air–sea gas flux model (Fairall et al. 2000; Hare et al. 2004; Blomquist et al. 2006) incorporates the influence of bubble bursting in whitecaps through the use of Woolf's (1997) model of bubble-mediated gas transfer; Woolf's model has yet to be tested against observations, however.

Many of the processes affecting gas exchange also have a controlling influence on the production of aerosol from sea spray (Monahan and O'Muircheartaigh 1986; Mårtensson et al. 2003). Sea salt aerosol is the dominant scatterer of solar radiation over the open ocean under clear skies (Haywood et al. 1999), significantly contributing to the global aerosol optical depth (O'Dowd and de Leeuw 2007) and significantly influencing cloud microphysics and chemistry (O'Dowd et al. 1999), particularly that of marine stratocumulus—one of the largest sources of uncertainty in current climate models. The full range of sea spray source functions proposed in the literature spans six orders of magnitude (Andreas 2002), although most recent estimates converge to within about one order of magnitude (Clarke et al. 2006).

AFFILIATIONS: Brooks, Bloom, Brooks, Lingard, McQuaid, Norris, Smith, and Smith—University of Leeds, Leeds, United Kingdom; Yelland, Moat, Pascal, Prytherch, Srokosz, and Taylor—National Oceanography Centre, Southampton, United Kingdom; Upstill-Goddard and Salter—University of Newcastle, Newcastle upon Tyne, United Kingdom; Nightingale, Archer, Beale, Dixon, Goldson, Hardman-Mountford, Liddicoat, Moore, and Stephens—Plymouth Marine Laboratory, Plymouth, United Kingdom; d'Asaro and McNeil—Applied Physics Laboratory, University of Washington, Seattle, Washington; Beatty and DeGrandpre—University of Montana, Missoula, Montana; Blomquist and Huebert—University of Hawaii at Manoa, Hawaii; Cluderay and Zemmelink—Royal Netherlands Institute for Sea Research (NIOZ), Texel, The Netherlands; Coles, Hsueh, and Leighton—University of Southampton, Southampton, United Kingdom; Dacey—Woods Hole Oceanographic Institution, Woods Hole, Massachusetts; Drennan, Rebozo, and Sahlee—Rosenstiel School of Marine and Atmospheric Science, University of Miami, Miami, Florida; Gabriele—National Water Research Institute, Environment Canada, Burlington, Ontario, Canada; Horn—University of Rhode Island, Kingston, Rhode Island; de Leeuw—Finnish Meteorological Institute and University of Helsinki, Finland; Neill and Skjelvan—Bjerknes Centre for Climate Research, University of Bergen, Norway; O'Doherty, Walsh, and Young—University of Bristol, Bristol, United Kingdom; Schuster and Telszewski—University of East Anglia, Norwich, United Kingdom; Slagter—University of Groningen, Groningen, The Netherlands; Ward—University of Galway, Galway, Ireland; Woolf—UHI Millennium Institute, Thurso, United Kingdom
ADDITIONAL AFFILIATION: de Leeuw—TNO B&O, Utrecht, The Netherlands
A supplement to this article is available online (10.1175/2008BAMS2578.2)
CORRESPONDING AUTHOR: Ian M. Brooks, Institute for Climate and Atmospheric Science, School of Earth and Environment, University of Leeds, Leeds LS2 9JT, United Kingdom
E-mail: i.brooks@see.leeds.ac.uk

The abstract for this article can be found in this issue, following the table of contents.
DOI:10.1175/2008BAMS2578.1

In final form 22 August 2008

Almost all sea spray source functions have been derived via indirect methods, relying on assumptions that are difficult to verify. Only a handful of recent studies have attempted direct eddy covariance measurements of the flux (Nilsson et al. 2001; Geever et al. 2005; de Leeuw et al. 2007; Norris et al. 2008). Again, the relative influence of the various forcing processes is largely unknown.

THE FIELD PROGRAMS. The HiWASE, SEASAW, and DOGEE field programs share a common goal: to understand the processes controlling physical exchanges at the air–sea interface and to extend measurements of gas transfer to high wind speeds; see the sidebar for a summary of specific objectives of the projects. Next, we discuss their approaches to meeting these objectives.

PROJECT OBJECTIVES

Common Objectives

- Establish the effect of various forcing parameters on the gas transfer velocities and improve their parameterization.
- Relate the gas transfer velocity to forcing parameters other than wind speed (sea state, whitecap coverage, wave breaking, rain, and friction velocity).
- Investigate wave breaking and whitecap production coincident with air–sea flux measurements to increase understanding and improve parameterization of both whitecap production and air–sea fluxes.
- Measure air–sea fluxes of CO_2, sensible and latent heat, and momentum by both direct eddy covariance and inertial dissipation techniques where appropriate.
- Quantify flow distortion biases in the direct flux measurements through the comparison of eddy correlation latent heat fluxes to the inertial dissipation latent heat fluxes after the latter have been corrected using computational fluid dynamics and correct other direct fluxes by analogy.

SEASAW

- Determine the sea spray source function via the direct eddy covariance method.
- Investigate the production and fate of sea spray aerosol particles very close to the ocean surface by means of 10-Hz optical particle counter observations and relate these measurements to those of subsurface bubble populations obtained via a bubble imaging system.
- Use a single particle aerosol mass spectrometer and associated instruments to study the composition of individual aerosol particles as a means of source apportionment and to investigate interactions between the sea spray aerosol and other aerosol and gaseous components.

HiWASE

- Produce a dataset of unprecedented size and detail by instrumenting a ship to obtain flux measurements continuously for three years, under a variety of conditions including high wind speed events.
- Obtain a comprehensive sea-state description by combining data from the 1D SBWR system with the directional information from the WAVEX wave radar system.
- Extend the parameterization of the gas transfer velocity to wind speeds more than 15 m s^{-1}.

DOGEE

- Carry out dual-tracer (^{3}He and SF_6) release experiments to derive estimates of the gas transfer velocity.
- Examine the effect of surfactant on k_w, sea-state, and near-surface turbulence.
- Make direct estimates of DMS fluxes by eddy covariance using an APIMS.
- Collect detailed profiles of surfactant, tracers, and other dissolved gases in the uppermost 2 m of the water column.
- Simultaneously record (using video) and measure (using capacitance wave wires) whitecap coverage and wave breaking and develop an improved parameterization of wave breaking.
- Quantify the bubble populations produced by breaking waves both at the sea surface and beneath it using acoustic methods.
- Use gradient flux and relaxed eddy accumulation techniques for measuring DMS fluxes and extend these techniques to other gases for which diffusivity characteristics are well known (methyl halides).
- Develop and deploy a sampling system for the collection of water samples for dissolved gas analysis from the sea surface microlayer.
- Determine spatial and temporal variability of biological methanol uptake, including fine-scale variability in the upper 2 m of the water column using the NSS; assess the relationship between heterotrophic bacterial production and rates of methanol uptake in the euphotic zone; and compare heterotrophic bacterial production and biological methanol uptake.

All three studies included direct eddy covariance measurements of the CO_2 flux, along with those of water vapor, heat, and momentum, and measurements of the wave spectrum, whitecap fraction, air–sea CO_2 partial pressure difference (ΔpCO_2), and mean meteorological conditions. SEASAW additionally encompassed eddy covariance measurements of the sea-spray aerosol flux, while DOGEE included direct measurements of the DMS flux and measurements of gas transfer from tracer release experiments. A brief summary of each project is given below; details of the instrumentation used are given online (http://dx.doi.org/10.1175/2008BAMS2578.2).

SEASAW and DOGEE both focused on process studies incorporating a wide range of measurements and requiring the facilities of a dedicated research vessel. These projects involved a total of three research cruises in the northeast Atlantic on board the RRS *Discovery*. A joint cruise off the west coast of Scotland, D313, from 7 November to 2 December 2006 targeted high wind conditions (Upstill-Goddard et al. 2007a). During the event, the winds proved to be too high—one of the worst series of storms on record resulted in conditions too severe to conduct most of the required operations and very few measurements were obtained. SEASAW made a second cruise, D317 (Brooks et al. 2007), between 21 March and 12 April 2007, again targeting high wind conditions. The DOGEE project conducted a final cruise, D320 (Upstill-Goddard et al. 2007b), between 16 June and 17 July 2007, this time focusing on the influence of near-surface gradients and surfactants under lower wind conditions. HiWASE (Yelland and Pascal 2008) adopted a very different approach to the other two studies, furnishing the Norwegian weather ship *Polarfront* with a more limited set of instrumentation but one capable of operating autonomously over a period of several years. This approach allows for the collection of a much larger dataset than is possible from typical research cruises, and it enables relatively infrequent extreme conditions to be sampled extensively enough to provide robust statistics. A map showing cruise locations is given in Fig. 1.

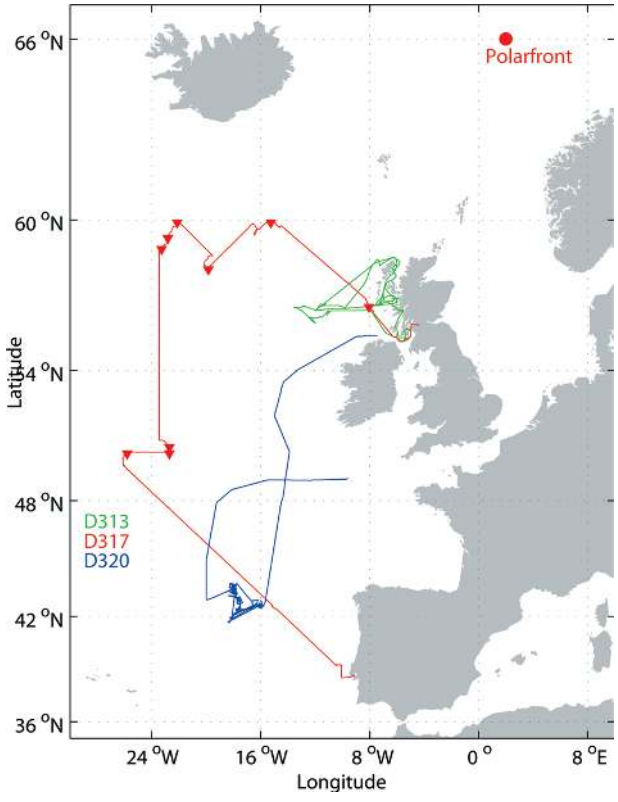

Fig. 1. Cruise tracks for SEASAW (D313 and D317) and DOGEE (D313 and D320), and the location of the *Polarfront* used by the HiWASE project. Red triangles indicate the measurement stations and buoy deployment locations during D317.

HiWASE. The *Polarfront* is the world's last weather ship. It is run by the Norwegian Meteorological Institute (DNMI) and operates year-round at Station Mike in Norwegian Sea (66°N, 2°E), a region that experiences both large CO_2 fluxes and frequent high-wind events. In September 2006, the National Oceanography Centre, Southampton (NOCS) equipped the *Polarfront* with an automated system for the direct measurement of air–sea fluxes: AutoFlux (Yelland et al. 2007b, 2009). The air and surface water partial pressures of CO_2 are measured by an IR-based system (Pierrot et al. 2009) installed by the Bjerknes Center for Climate Research (BCCR), University of Bergen. The *Polarfront* is fitted with a shipborne wave recorder (SBWR) (Tucker and Pitt 2001; Holliday et al. 2006) that provides 1D wave height spectra but no directional information. HiWASE supplemented this with a commercial wave radar, WAVEX, that provides 2D wave spectra from an X-band marine radar. The two wave measurement systems are complementary and provide a comprehensive sea-state dataset (Yelland et al. 2007a). It is believed this is the first time these two instruments have been deployed together for an extended period. Wave breaking can be identified from "sea spikes" in the raw wave radar images, while whitecap fraction is derived from photographic images obtained at 5-min intervals from two digital cameras installed on the bridge. Mean meteorological measurements are provided by the DNMI instrumentation, supplemented with sensors for downwelling longwave and shortwave radiation, IR sea surface temperature, and wet- and dry-bulb air

temperature. Important for a long-term autonomous system, an Iridium satellite link provides daily status and data summaries (www.noc.soton.ac.uk/ooc/CRUISES/HiWASE/OBS/data_intro.php) and allows for some remote control of the data logging system. HiWASE will continue collecting measurements until at least summer 2009.

SEASAW. The primary focus of SEASAW was to make direct eddy covariance measurements of both sea-spray aerosol and CO_2 fluxes. An AutoFlux system was installed with twin sets of sonic anemometers and LI-COR LI-7500 units on either side of the foremast platform (Fig. 2). A second flux system was installed at the top of the foremast extension, with the addition of a new high-frequency aerosol spectrometer, the Compact Lightweight Aerosol Spectrometer Probe (CLASP) (Hill et al. 2008). A suite of instruments measured the background aerosol spectra and composition. Near-surface measurements of aerosol and bubble spectra were made from a tethered buoy. One-dimensional wave spectra were obtained from an SBWR system, and whitecap fraction was determined from cameras identical to those on the *Polarfront* but with images captured at 30-s intervals. Carbon dioxide partial pressures in air and water were measured by infrared-based systems from the University of East Anglia (cruise D313) and the Plymouth Marine Laboratory (PML; cruises D313 and D317) (Hardman-Mountford et al. 2008).

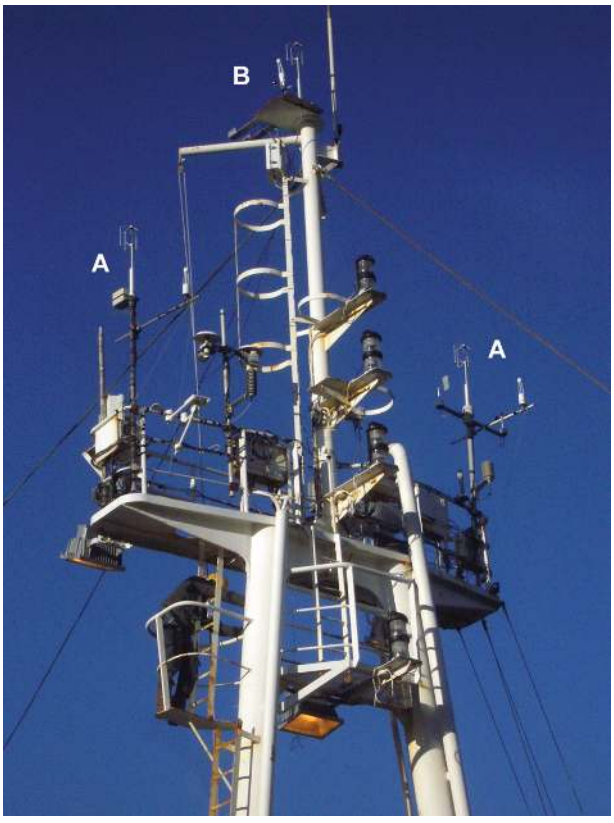

Fig. 2. The foremast of the RRS *Discovery* instrumented for the SEASAW cruises. (a) The AutoFlux instrumentation is located at either end of the foremast platform. (b) The Leeds flux instrumentation is located at the top of the mast extension.

DOGEE. The DOGEE project conducted the widest-ranging measurements of the three programs, focused around a dual-tracer (^{3}He and SF_6) release for measuring k_w (Watson et al. 1991). Multiple simultaneous direct flux measurements were also made: CO_2 fluxes by AutoFlux and from two air–sea interaction spar (ASIS) buoys (Graber et al. 2000) deployed within the tracer patches and a DMS flux system with inlet and sonic anemometer collocated at the top of the foremast extension. High-resolution dissolved DMS and SF_6 measurements were made in the near-surface water column to assess the role of near-surface gradients in air–sea exchange (Zemmelink et al. 2002). Such gradients are potentially significant for biologically active gases. Autonomous gas floats (d'Asaro and McNeil 2007) measured ocean boundary-layer concentration profiles and eddy covariance fluxes of O_2, N_2, and heat in the water column. Continuous underway measurements of dissolved O_2, N_2, and CO_2 were also made, along with discrete measurements of dissolved and gaseous oxygenated volatile organic compounds. In addition to wave data from the SBWR, more detailed measurements were made from multiple capacitance wave wire systems: one on each ASIS buoy and one on a spar buoy deployed by NOCS to study wave breaking, whitecapping, and bubble populations. Whitecap imaging cameras were again installed on the bridge.

MEASUREMENT HIGHLIGHTS.

Dual Tracer Release. A gas exchange velocity can be determined from the rate of change in concentration of a tracer labeling a patch of seawater (Watson et al. 1991; Nightingale et al. 2000). During DOGEE cruise D320, 6.5 m^3 of seawater was saturated with SF_6 and ^{3}He and released as three distinct patches in rapid succession, initially covering areas of 4, 2, and 1 km^2, the smallest patch being overlaid with a surfactant. Drogued Lagrangian drifters were used to adjust the ship's track during release, to compensate for water mass movement, and to aid with patch relocation. Each drifter had Argos and radio communication and a vertical array of temperature/pressure loggers for estimating scales of internal waves, mixed layer

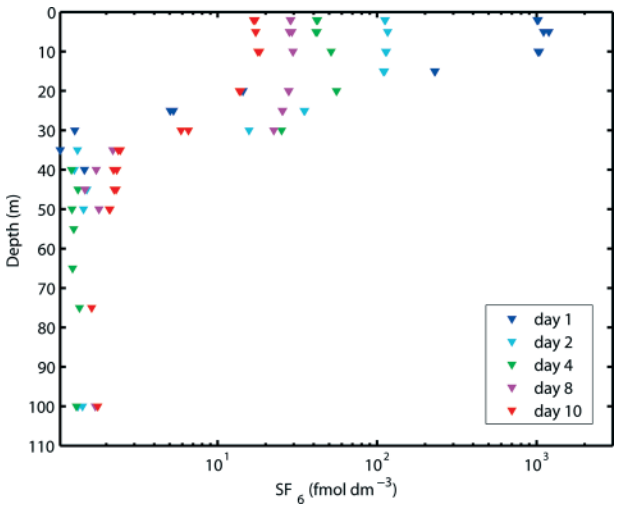

Fig. 3. Changes in SF_6 concentration in depth profiles from patch 2 in the days following the tracer release. Concentrations decrease rapidly as the patch spreads both horizontally and vertically and, to a lesser extent, as the gas diffuses across the air–sea interface. Note that background concentrations below the mixing layer are typically 1.5 fmol (i.e. 10^{-15} moles) per liter of seawater.

stratification, and temporal changes in mixed layer depths. Continuous underway mapping of surface water dissolved SF_6 (Upstill-Goddard et al. 1991) identified each of the three patch centers, where SF_6 and ^{3}He were periodically sampled from vertical hydrocasts. A total of 23 hydrocasts were made, each acquiring water samples at a minimum of 10 depths for SF_6 and 3 depths of ^{3}He. Example profiles of SF_6 concentrations shortly after tracer deployment are shown in Fig. 3.

Surfactant Releases. A unique experiment has been the deliberate release of a harmless surfactant (oleyl alcohol) onto the sea surface. The surfactant was initially laid over the smallest of the tracer patches as a series of parallel lines spaced 125 m apart across a region 2.5 km × 2.5 km centered on the 1 km × 1 km tracer patch; these then spread to form a continuous patch. The damping of sea surface capillary waves as the surfactant was deployed is clearly visible in Fig. 4. Comparison of k_w estimates from the surfactant-free and surfactant-covered tracer patches under similar wind and wave fields will attempt to provide the first direct assessment of the surfactant effect on air–sea gas exchange as measured by the dual tracer technique.

In addition to the release over a $SF_6/^3$He patch, three additional surfactant releases were carried out. The first was a deployment ahead of one of the ASIS buoys once both buoys had progressed substantially downwind of the initial $SF_6/^3$He patches in which they were deployed and were following approximately parallel headings ~20 km apart. The two sets of ASIS measurements will be examined to identify the effects of surfactant damping on the direct flux estimates. The second release took place around the NOCS buoy to examine surfactant effects on the wave field. The third release took place within an area of high ambient DMS off the west coast of Ireland to examine the influence of the surfactant on the DMS flux.

SURFACE MICROLAYER MEASUREMENTS.

The sea surface microlayer (SML) is traditionally defined as the uppermost millimeters of the water column and is characterized as a region where physical, chemical, and biological properties are most altered relative to subsurface water (Liss et al. 1997). The formation of the SML results from organic matter concentrated at the air–sea interface by numerous physical and biological processes—such as diffusion, turbulent mixing, transport by rising bubbles or buoyant particles and in situ production—while biological and photochemical mineralization and vertical transport are considered the major loss mechanisms of SML material (Liss et al. 1997).

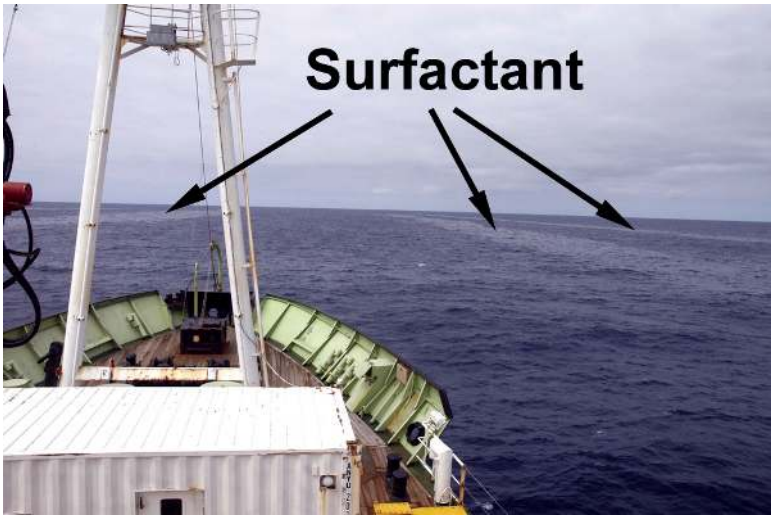

Fig. 4. During deployment of the surfactant patch, the lines along which it has been initially laid are clearly visible by the suppression of capillary waves.

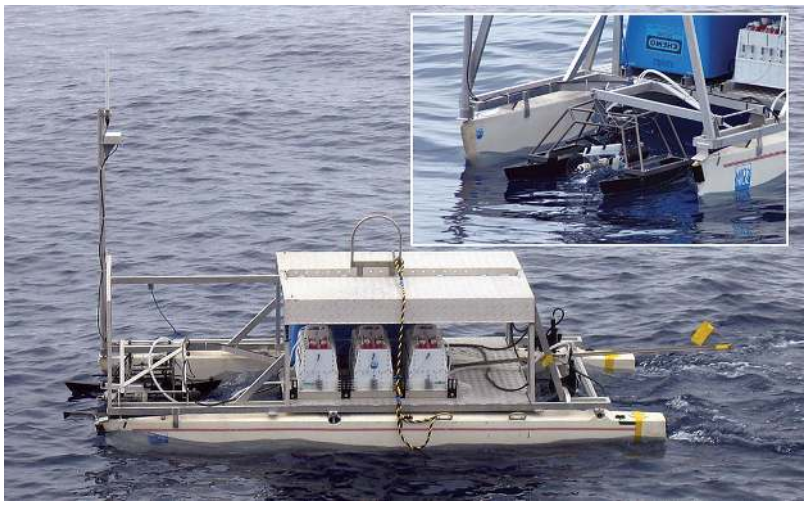

Fig. 5. The remote-controlled catamaran and (inset) close-up of the surface skimmer operating during the second DOGEE cruise.

Measurements of production, destruction, and transport processes in the SML of most organic compounds and trace gases are limited. To gain more insight into these processes, the microlayer and the underlying water column were sampled during the second DOGEE cruise by a surface skimmer. This consists of a rotating glass cylinder supported by a remotely controlled catamaran (Fig. 5); this collects a film of water 50-μm thick by adhering to the drum. The aqueous film is wiped off the cylinder and collected into bottles using peristaltic pumps, minimizing the loss of volatiles to the atmosphere that were reported in previous studies (Frew et al. 2002; Zemmelink et al. 2005). Samples are subsequently analyzed in the laboratory. Unlike common alternative techniques, such as manual submersion of screens or glass plates used for sampling biota and surfactants (Agogué et al. 2004), the skimmer provides accurate control of the sampling depth and avoids contamination of SML samples by subsurface water.

Microlayer and subsurface water samples were routinely collected at intervals throughout the cruise for surfactant activity measurements and for bacterial community analysis, both within and outside the artificial surfactant patches. Microlayer samples for surfactant analysis were collected with a Garrett screen and a glass plate, whereas bacterial samples were collected on polycarbonate membranes and Sterivex filters. Contamination was avoided by sampling some distance off the ship from a rigid inflatable boat; additional Garrett screen samples were collected from over the side of the ship. Numerous near-surface profiles were also obtained using both a near-surface sampler (PML) and the surface skimmer on the remote-controlled catamaran. Sulfur profiles from 2-m depth to the surface of the water column show a decrease of the volatile DMS in the microlayer that could be caused by outgassing from the water column (Fig. 6). Total dimethylsulfoniopropionate (DMSP) showed a small decrease toward the water surface; in contrast, total dimethylsulfoxide (DMSO) showed an increase in the surface microlayer compared to the deeper water column. This gradient indicates that most DMSO(t) is formed and trapped at the water surface, where photooxidation might enhance the conversion of DMS to DMSO.

MIXED LAYER PROFILING. Gas exchange at the surface depends upon processes within the ocean mixed layer as well as atmospheric forcing; to investigate these, an autonomous float (d'Asaro 2003) was deployed during the DOGEE cruise D320 to measure profiles of temperature, gas concentration, and turbulent exchange. The float made daily slow profiles from the surface to about 110 m to measure the mean properties of the water column. Between profiles, it acted as a fully 3D Lagrangian tracker, following turbulent eddies in the mixed layer. Figure 7 shows cross sections of density and gas concentration for a 2-week period, along with mixed layer depth. A storm disrupts the gradual seasonal trends between days 180 and 183, deepening the mixed layer. During this period, profiles were omitted and the float was

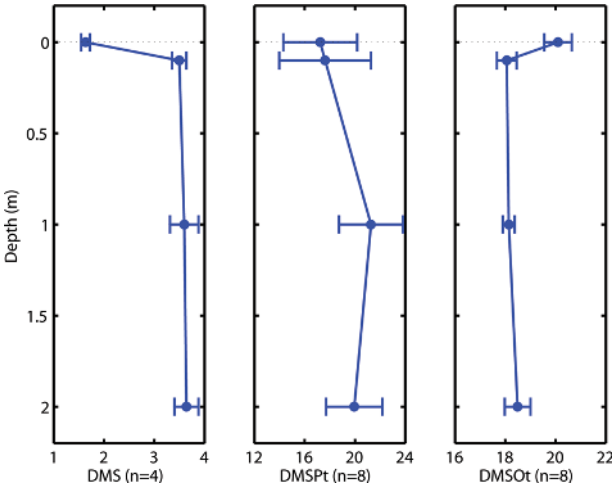

Fig. 6. Near-surface profiles of DMS, DMSP, and DMSO obtained by the catamaran.

left in Lagrangian mode. During weak winds before the storm, O_2 saturation was forced by the seasonal warming of the mixed layer, driving a net flux to the atmosphere; during the storm, float covariance estimates showed that O_2 was forced into the water. After the storm, there was a strong increase in O_2 concentration at a depth of 25–50 m. The lack of a corresponding change in N_2, which can be considered a proxy for abiotic O_2 associated with entrainment fluxes and air–sea exchange, suggests that this results from a biological process—a phytoplankton bloom triggered by the mixing up of nutrients during the storm.

Figure 8 shows the vertical motion of the float and the perturbation of O_2 concentration about its profile mean during part of the storm. The positive perturbations of O_2 in the downward arms of the mixed layer eddies indicates an air–sea flux into the ocean. A detailed analysis, using the technique of d'Asaro (2003) gives a flux estimate of 787 nmol m^{-2} s^{-1} with an uncertainty of about 30%. The reversal of the sign of the O_2 flux during the storm suggests the importance of bubble dissolution processes for air–sea gas fluxes.

DIRECT FLUX MEASUREMENTS. The direct flux measurements undertaken during UK–SOLAS provide a substantial dataset; notable highlights are the extension of gas flux measurements to mean U_{10} values of 15 m s^{-1} during DOGEE, 18 m s^{-1} during SEASAW, and 28 m s^{-1} during HiWASE—higher than any previously published measurements—and the first size-segregated direct aerosol flux measurements over the open ocean. Eddy covariance flux measurements are extremely challenging at sea as a result of the need to determine the motion and attitude of the platform and to remove these effects from the measured wind components (Edson et al. 1998; Brooks 2008). Flow distortion around the ship can also introduce significant biases and must be corrected (Yelland et al. 1998, 2002). This is illustrated in Fig. 9, which shows the transfer coefficient for the momentum flux (CD10n) obtained from the HiWASE sensors on the *Polarfront*. The data are separated into two classes: (1) when the wind was blowing onto the ship's bow and flow distortion effects are expected to be small (Yelland et al. 2009) and (2) when the wind was blowing onto the beam and the effects are

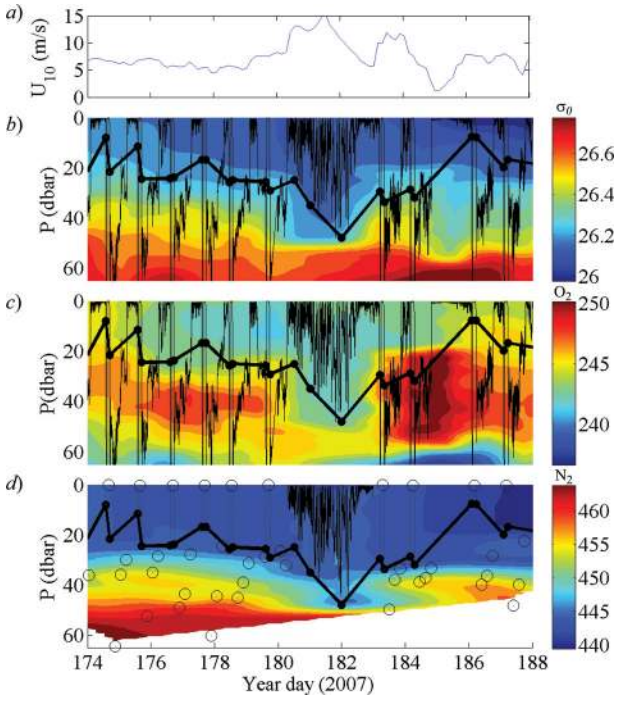

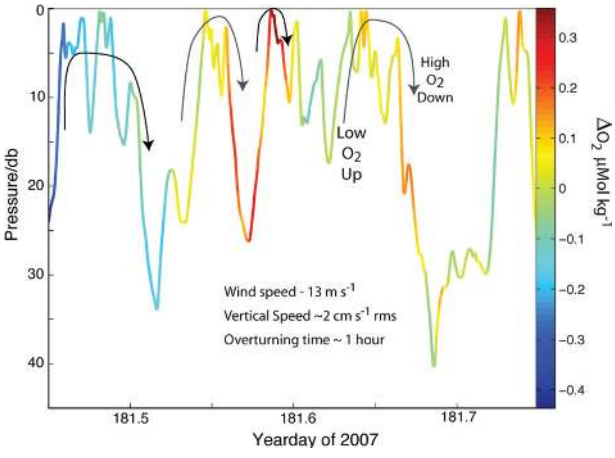

FIG. 7 (LEFT). Meteorological and water column measurements at the float, showing (a) wind speed U_{10}, (b) seawater potential density σ_0 versus hydrostatic pressure P, (c) dissolved O_2 concentrations, and (d) dissolved N_2 concentrations. The locations of the surface/pycnocline N_2 sampling are shown (open circles) in (d), along with positions of mixed layer values (small black dots arranged in vertical lines throughout the mixed layer) for contouring purposes. The depth trajectory of the float (thin overlaid black lines) is shown in (b)–(d), along with mixed layer depth estimates (large black dots connected by thick black line). Note that N_2 data are available continuously in the mixed layer during the storm, and that O_2 has significantly greater depth/time sampling resolution than N_2.

FIG. 8 (RIGHT). Depth–time trajectory of the Lagrangian float during part of the storm. The line color represents the deviation of the measured O_2 concentration from its average profile smoothed over about 300 s. Note the persistent pattern of higher O_2 during downward motion than during upward motion. This pattern indicates a net flux of O_2 into the ocean from the atmosphere.

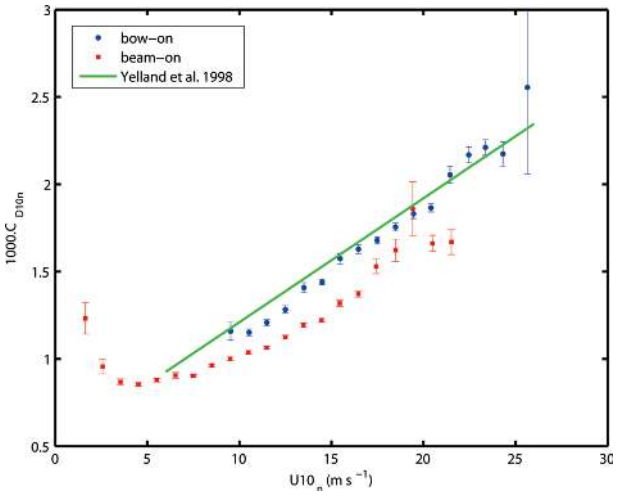

FIG. 9. Neutral drag coefficients determined from bow-on (blue) and beam-on (red) wind measurements on the *Polarfront* averaged in 1 m s^{-1} wind speed bins; error bars indicate the standard error about the means. The relationship from Yelland et al. (1998) is shown for comparison. The beam-on results are very obviously biased low.

expected to be large. The beam-on data are biased significantly low. An ongoing part of our analysis is to assess the influence of flow distortion on eddy covariance measurements and to develop procedures to correct the resulting biases.

Gas Fluxes. A total of five independent eddy covariance systems for measurement of gas fluxes have been used during these studies—two independent CO_2 flux systems operated during each of the *Discovery* cruises, along with the DMS flux system during the second DOGEE cruise. Analysis of the CO_2 measurements is not yet sufficiently advanced to present any results. This is due in large part to the discovery of both significant noise and a small bias introduced into the high-rate CO_2 flux estimate by the mechanical deformation of the Licor 7500 sampling head under the accelerations induced by ship motion (Yelland et al. 2009). Procedures to correct for this contamination are being evaluated. Mean forcing conditions and bulk estimates of the CO_2 flux for a 100-day record from HiWASE are shown in Fig. 10. Bulk fluxes are shown based on limiting values of the transfer velocity. Substantial differences between them are seen during high wind events; the average fluxes during the 100-day period are –2.77 μmol m^{-2} yr^{-1} (using Liss and Merlivat 1986) and a factor of 1.8 higher at –5.05 μmol m^{-2} yr^{-1} (using McGillis et al. 2001).

Direct DMS fluxes were measured using an atmospheric pressure ionization mass spectrometer (APIMS) (Huebert et al. 2004). The APIMS was located in a container on the foredeck with a sample drawn from an inlet collocated with a sonic anemometer at the top of the foremast extension. A total of 368 flux estimates were obtained from hour-long intervals, 164 of which also included one or more measurements of seawater DMS, enabling the computation of k_{DMS}. Figure 11 shows some results in the region of a phytoplankton bloom west of Ireland; it is clear that the DMS flux is highly variable as a result of variations in both seawater DMS concentration and wind speed. Preliminary exchange velocities are far less dependent on local wind speed than predicted by the commonly used models, where k_w increases as the square or cube of wind speed increases. The preliminary analyses show variable results in the surfactant patch; there appears to be a reduced transfer

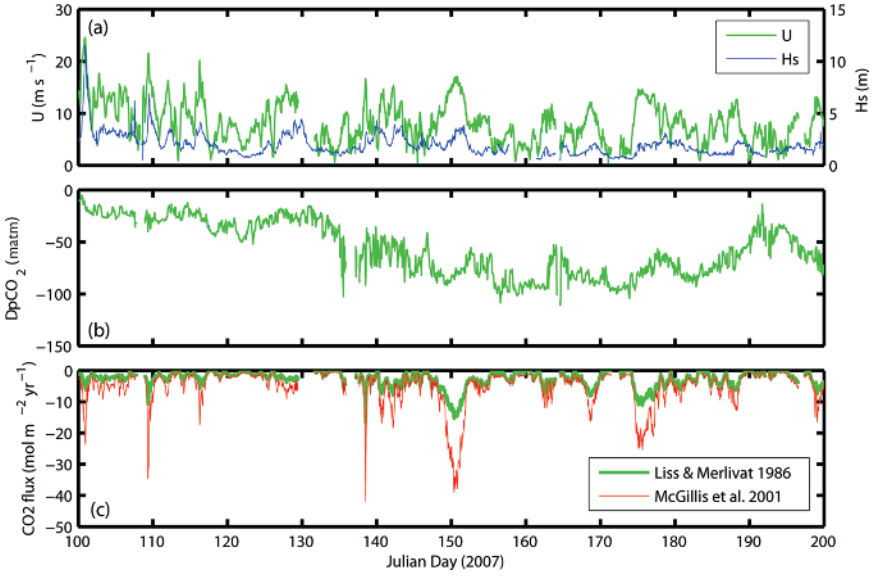

FIG. 10. A 100-day time series of HiWASE measurements on the *Polarfront*: (a) mean wind speed *U* and significant wave height H_s; (b) air–sea difference in pCO_2; (c) bulk estimates of the CO_2 flux from parameterizations that span the range of published values for transfer velocity (Liss and Merlivat 1986; McGillis et al. 2001). The mean fluxes over the 100 days are −2.77 (Liss and Merlivat 1986) and −5.05 μmol m^{-2} yr^{-1} (McGillis et al. 2001).

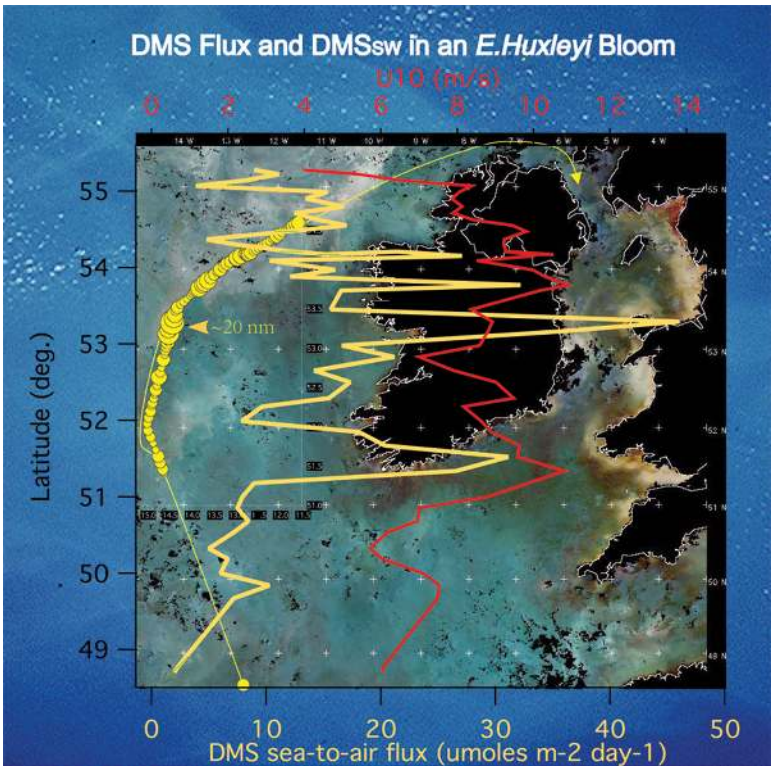

Fig. 11. DMS during a transit through an *E. huxleyi* bloom west of Ireland. The size of the yellow circles represents the seawater DMS concentration; the thick yellow line is the eddy covariance DMS flux. The red line is the mean 10-m wind speed. A surfactant patch was laid at 54.2°N.

rate within the patch laid at 54.2°N. However, other patches show no obvious effect or even a slightly higher transfer velocity for DMS. Firm conclusions await the completion of a more rigorous analysis of all the measurements.

Aerosol Fluxes. Eddy covariance flux measurements require sensors with a response of better than ~3 Hz. Few traditional aerosol instruments are adequate. A new compact weatherproof aerosol spectrometer probe (CLASP; Hill et al. 2008), developed specifically for making eddy covariance flux measurements, was used during SEASAW. Small enough to collocate with a sonic anemometer, CLASP provides a 16-channel aerosol-size spectrum for particles with radii between about 0.12 and 9.25 μm. An earlier version made the first fully sized segregated eddy covariance sea-spray flux measurements at a coastal site (Norris et al. 2008). The aerosol flux measurements made during SEASAW are the first to be made over the open ocean. They show much greater variability than is observed for other fluxes, both between the flux estimates from individual data records and in the contribution to individual estimates from different turbulence scales within a given record (Fig. 12). This is a result of the surface source of particles not being continuous but discrete and widely spaced patches—individual whitecaps. An implication of this is that much larger volumes of data are required to achieve the same confidence levels as for fluxes of momentum, heat, or moisture.

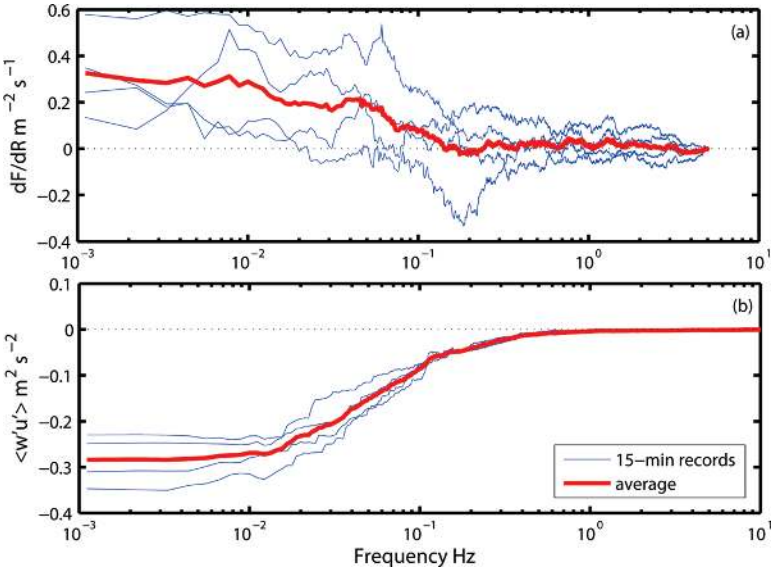

Fig. 12. Ogive functions showing the cumulative contributions with decreasing frequency (increasing eddy scale) to the fluxes of (a) particles (R = 0.3 μm) and (b) wind stress for several consecutive 15-min records (blue lines) and their averages (red lines). The variability between records is much greater for the particle flux, which also shows far greater variation in the contribution to the flux with frequency. The averaged curves, however, show that the turbulence scales contributing to the particle flux are the same as those for the wind stress.

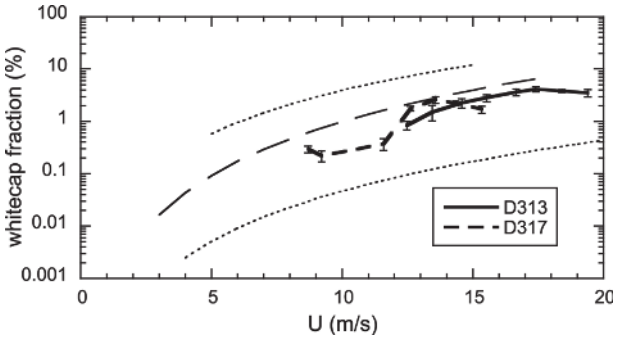

Fig. 13. Whitecap coverage as a function of wind speed. The thin dotted lines indicate the range of results previously found by a large number of photographic studies (Anguelova and Webster 2006). The thin dashed line indicates the open-ocean relationship of Monahan and O'Muircheartaigh (1980). The thick lines show initial results from a few days of D313 and D317 data as indicated in the key. Error bars indicate the standard error.

WAVE BREAKING AND WHITECAP MEASUREMENTS. Whitecap coverage estimates were obtained from images of the sea surface taken during daylight hours using two bridge-mounted digital cameras. Images were taken every 30 s at a resolution of 5 Mp during both the DOGEE and SEASAW cruises. Slower sampling rates and lower resolutions were used during HiWASE, since the cameras were serviced only every two or three months rather than every day. A grayscale image analysis similar to that employed by Stramska and Petelski (2003) was used to isolate whitecaps from the surrounding sea. Initial results show an increase of whitecap fraction with wind speed (Fig. 13) similar to that from the open-ocean study of Monahan and O'Muircheartaigh (1980). Analysis of the HiWASE images will provide whitecap data at wind speeds of up to 28 m s^{-1}. When complete, the whitecap data from all three UK–SOLAS cruises will be used to investigate parameterizations of whitecap coverage in terms of mean meteorological variables and sea state and the effect of whitecap fraction on the CO_2 flux.

Wave Breaking. Measuring the properties of breaking waves and whitecap properties in the open ocean is extremely challenging, and there have been few measurements to date. To address these issues, an autonomous, free-floating spar buoy was designed by NOCS to measure the properties of both waves and the bubbles resulting from wave breaking (Fig. 14). The spar is 11 m in length and floats 80% submerged. It has an onboard battery bank and custom-built data acquisition and control system and operates autonomously, drifting free of the ship. An Argos system sends the buoy position to the ship every hour and is also used for radio directional finding to aid recovery. Three 4-m-long capacitance wave wires measure the surface elevation with respect to the spar with a resolution of 3 mm. The motion of the buoy over long waves and swell was determined from a motion-sensing package that measured three-axis accelerations and compass heading. Wave wire and motion data were sampled at 41 Hz (except for the heading, sampled at 8 Hz), providing the information required to calculate wave heights and slopes. A waterproof sphere at the top of the spar housed digital still and video cameras focused on the surface around the wave wires, along with the wave wire electronics. Figure 15 shows a 4-s section of surface elevation data from one wire, along with the temporal wave "slope" (i.e., the time derivative of the elevation; Longuet-Higgins and Smith 1983). A breaking wave is seen just before 564 s; this event was also captured by the cameras on the buoy (Fig. 16).

Bubble Measurements. Bubble populations under breaking waves can total millions per cubic meter and contain bubbles ranging in radius from microns to centimeters. Of the available techniques for measuring such populations, acoustic methods

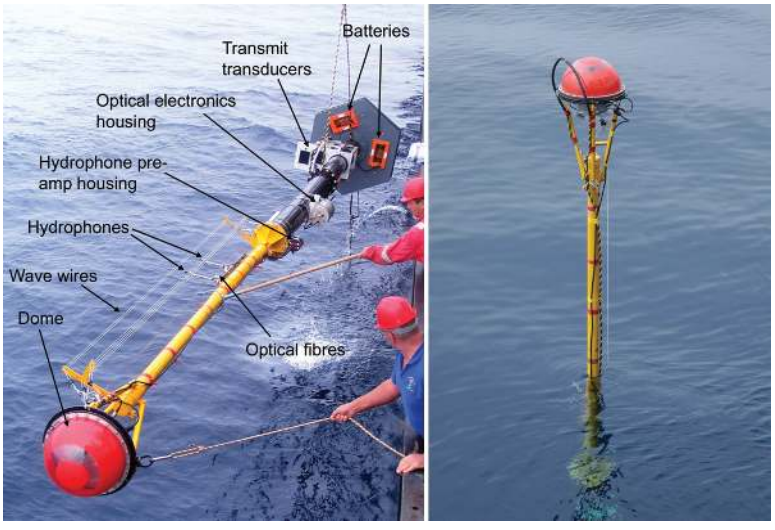

Fig. 14. Photographs of the spar buoy (bottom left) during deployment with key features labeled and (bottom right) floating free.

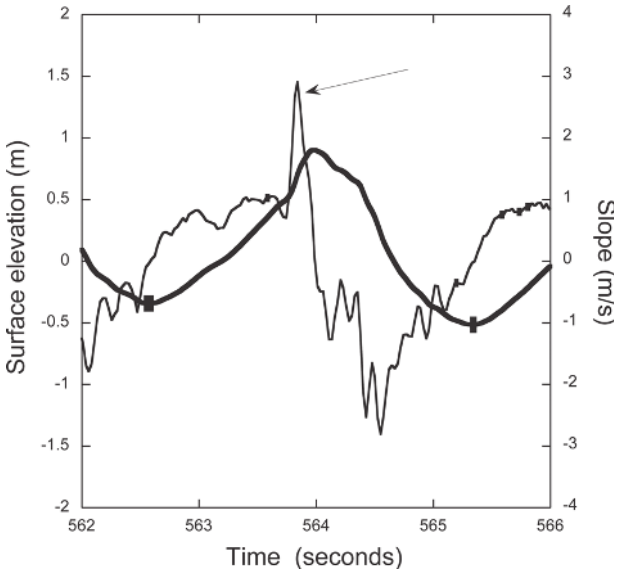

Fig. 15. Four-second time series of surface elevation (thick line) and slope (thin line) from one of the wave wires (note separate *y*-axis scales). A breaking wave is indicated by the arrow.

are the most applicable (Leighton 2004, 2007); however, they can contain ambiguities that require a cross-check against an independent measurement (Leighton et al. 1996, 1997; Vagle and Farmer 1998). The spar buoy was equipped with two acoustic and one optical system for determining the bubble population. The optical system used three fiber-optic tips mounted along the buoy. As bubbles pass over the tips, a change in light intensity is measured. Each bubble generates a transient with a magnitude, duration, and rise time related to the size of the bubble (Fig. 17); the bubble population can be inferred from the time series (Cartellier and Achard 1991; Blenkinsopp and Chaplin 2007). The two acoustic systems provide complementary information on the bubble plumes advecting past the buoy. The first acoustic system provides an estimate of the bubble-size spectra (Fig. 18) from a train of acoustic pulses (3–197 kHz), transmitted from near the base of the spar and measured by hydrophones at three locations between the transmitter and the surface. The bubble population is inferred from the additional acoustic attenuation as a result of the bubbles between pairs of hydrophones (Leighton et al. 2004; Coles and Leighton 2007). The second acoustic system monitors the signal backscattered from the bubble cloud by an upward-looking sonar and therefore giving an estimate of the overall size and shape of the bubble cloud as it is advected past the buoy.

Bubble spectra were also obtained during SEASAW (Fig. 18), from a video-based bubble imaging system (Leifer et al. 2003; de Leeuw and Cohen 2001) mounted on the underside of a small tethered buoy at a depth of 0.4 m. CLASP units mounted on the buoy at approximately 0.5 and 1 m above the surface allow the aerosol spectra within plumes originating over individual whitecaps to be determined. A motion pack on the buoy allows the high-rate aerosol spectra to be interpreted with respect to the buoy's position on the waves.

SUMMARY. The UK–SOLAS surface exchange field programs have provided a wealth of new data. These highlights include the following measurements:

- The first multiple patch dual-tracer release experiment;
- The first deliberate surfactant release experiments;
- The extension of measurements for direct gas flux estimates up to 10-m wind speeds of 28 m s^{-1};
- The ongoing acquisition of a continuous, multiyear set of direct gas flux measurements over the open ocean;
- The first direct eddy covariance measurements of fully size-resolved sea-spray aerosol fluxes over the open ocean;
- Simultaneous measurement of air–sea fluxes of multiple trace gases by multiple techniques;
- Comprehensive sea-state and whitecap measurements from buoy and ship systems simultaneous with gas and aerosol flux measurements.

Fig. 16. A sequence of images from the still camera on the spar buoy; images are obtained at 0.4-s intervals. The breaking wave in Fig. 15 can be seen in the last two images.

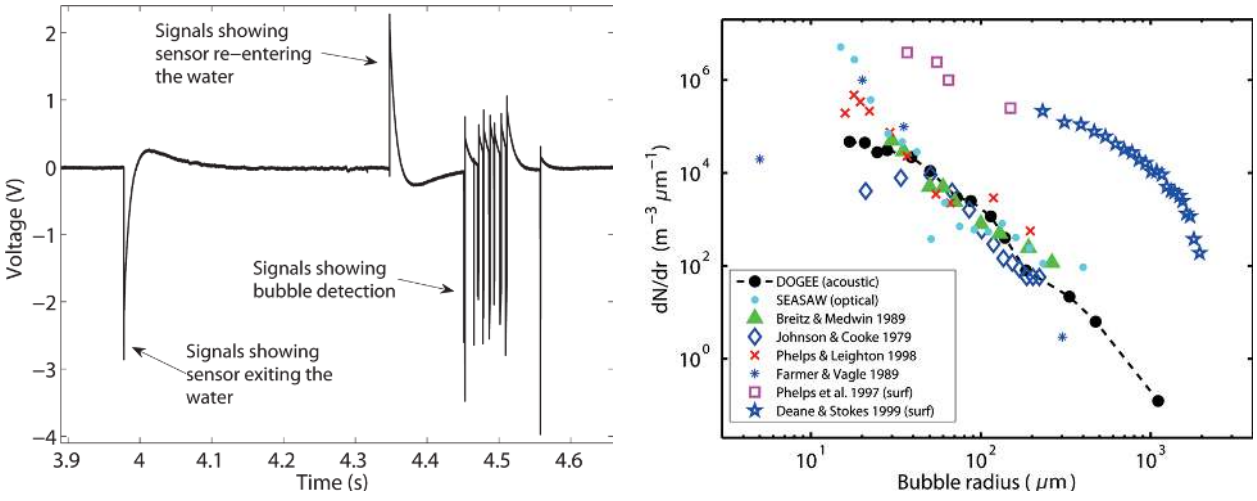

FIG. 17 (LEFT). A segment of the time series data from one of the fiber-optic sensors as a series of bubbles pass over it. At the start of the sequence, the fiber-optic sensor is initially submerged in the ocean. Then a passing wave causes the local sea level to dip, exposing the fiber tip to air from time (3.97–4.34 s), when the tip is again submerged by the wave. After this a sequence of transients, each indicating the detection of a bubble at the fiber-optic tip, are detected. These data were obtained on cruise D320 at 14:12 GMT on 22 Jun 2007 (J173) at 43°42′N, 18°07′W. Wind speed: ~7 m s^{-1}; average wave height: ~1.9 m; water temperature: ~17°C. The average depth of the fiber-optic tip is 0.25 m.

FIG. 18 (RIGHT). Bubble-size spectra (number concentration per μm radius bin) from the acoustic system on the spar buoy (black circles). The symbols correspond to the bubble sizes that were resonant with the specific tones emitted. This population estimate represents the spatially averaged bubble density between two hydrophones, at mean depths of 0.93 and 2.67 m, over a period of 9 s obtained at 1826 GMT, 29 Jun 2007 (J180) at 43°5′N, 17°38′W (DOGEE cruise D320) with mean wind speed of 13 m s^{-1}, mean wave height 2.7 m, and water temperature ~17°C. A spectrum obtained by the bubble camera on the SEASAW tethered buoy on 31 Mar is also shown; the wind speed and wave heights are similar to the DOGEE case but the water temperature is colder at ~9°C. For comparison, numerous open-ocean spectra obtained using different acoustic techniques are shown (Breitz and Medwin 1989; Phelps and Leighton 1998; Farmer and Vagle 1989), along with one spectra obtained by an optical system (Johnson and Cooke 1979) and two spectra from the surf zone showing much higher bubble concentrations and measured by acoustic (Phelps et al. 1997) and optical techniques (Deane and Stokes 1999).

Analysis of the data is only beginning, and we look forward to the possibilities offered by such wide-ranging measurements. They will enable the assessment of the influence of most of the processes believed to affect gas exchange and sea spray aerosol production and the development of new parameterizations for use in climate models. The strong links between the three projects enhances their individual strengths, extending the range of measurement conditions, facilitating direct comparisons between multiple techniques, and enabling the truly interdisciplinary approach required to properly understand physical exchange at the air–sea interface.

ACKNOWLEDGMENTS. The UK–SOLAS projects were funded by the Natural Environment Research Council Grants NE/C001826/1 (HiWASE), NE/C001842/1 (SEASAW), NE/C001702/1 (DOGEE), and NE/E011489/1 (DMS Fluxes); and by NSF Grants ATM05-26341 (Hawaii), OCE-0623450 (Miami), and NSF-OCE 0549887/0834340/0550000 (APL-UW). We would like to thank the captains and crews of the RRS *Discovery* and the *Polarfront,* along with the technical support staff of NERC's National Marine Facilities for their support throughout all these projects. Thanks also to Knut Bjorheim of DNMI for permission to use the *Polarfront.* McNeil is Vice President and co-owner of Pro-Oceanus Systems, Inc. manufacturer of the GTD's used in this study.

REFERENCES

Agogué, H., and Coauthors, 2004: Comparison of samplers for the biological characterization of the sea surface microlayer. *Limnol. Oceanogr.: Methods,* **2,** 213–225.

Andreas, E. L., 2002: A review of the sea spray generation function for the open ocean. *Atmosphere–Ocean Interactions,* Vol. 1, W. Perrie, Ed., WIT Press, 1–46.

Anguelova, M. D., and F. Webster, 2006: Whitecap coverage from satellite measurements: A first step toward mod-

eling the variability of oceanic whitecaps. *J. Geophys. Res.,* **111,** C03017, doi:10.1029/2005JC003158.

Asher, W. E., and Coauthors, 1995: Measurement of gas transfer, whitecap coverage, and brightness temperature in a surf pool: An overview of WABEX-93. *Air–Water Gas Transfer*: *Selected Papers from the Third International Symposium on Air–Water Gas Transfer,* B. Jähne and E. C. Monahan, Eds., AEON Verlag and Studio, 204–216.

——, A. T. Jessup, and M. A. Atmane, 2004: Oceanic application of the active controlled flux technique for measuring air–sea transfer velocities of heat and gases. *J. Geophys. Res.,* **109,** C08512, doi:19.1029/2003JC001862.

Blenkinsopp, C. E., and J. R. Chaplin, 2007: Void fraction measurements in breaking waves. *Proc. Roy Soc. London,* **A463,** 3151–3170.

Blomquist, B. W., C. W. Fairall, B. J. Huebert, D. J. Kieber, and G. R. Westby, 2006: DMS sea–air transfer velocity: Direct measurements by eddy covariance and parameterization based on the NOAA/COARE gas transfer model. *Geophys. Res. Lett.,* **33,** L07601, doi:10.1029/2006GL025735.

Bock, E. J., T. Hara, N. M. Frew, and W. R. McGillis, 1999: Relationship between air–sea gas transfer and short wind waves. *J. Geophys. Res.,* **104** (C11), 25 821–25 831.

Brietz, N., and H. Medwin, 1989: Instrumentation for in situ acoustical measurements of bubble spectra under breaking waves. *J. Acoust. Soc. Amer.,* **86,** 739–743.

Brooks, I. M., 2008: Spatially distributed measurements of platform motion for the correction of ship-based turbulent fluxes. *J. Atmos. Oceanic Technol.,* **25,** 2007–2017.

——, and Coauthors, 2007: Sea Spray, Gas Fluxes and Whitecaps Study (SEASAW) Cruise D317: March 21–April 12 2007. Institute for Atmospheric Science, University of Leeds Report, 60 pp. [Available online at www.bodc.ac.uk/data/information_and_inventories/cruise_inventory/report/d317.pdf.]

Cartellier, A., and J. L. Achard, 1991: Local phase detection probes in fluid/fluid two-phase flows. *Rev. Sci. Instrum.,* **62,** 279–303.

Clarke, A. D., S. R. Owens, and J. Zhou, 2006: An ultrafine sea-salt flux from breaking waves: Implications for cloud condensation nuclei in the remote marine atmosphere. *J. Geophys. Res.,* **111,** D06202, doi:10.1029/2005JD006565.

Coles, D. G. H., and T. G. Leighton, 2007: Autonomous spar-buoy measurements of bubble populations under breaking waves in the Sea of the Hebrides. *Proc. Second Int. Conf. and Exhibition on Underwater Acoustic Measurements: Technologies and Results,* Heraklion, Crete, Greece, Foundation for Research and Technology, 543–548.

d'Asaro, E. A., 2003: Performance of autonomous Lagrangian floats. *J. Atmos. Oceanic Technol.,* **20,** 896–911.

——, and C. L. McNeil, 2007: Air–sea gas exchange at extreme wind speeds measured by autonomous oceanographic floats. *J. Mar. Syst.,* **66,** 92–109.

Deane, G. B., and M. D. Stokes, 1999: Air entrainment processes and bubble size distributions in the surf zone. *J. Phys. Oceanogr.,* **29,** 1393–1403.

de Leeuw, G., and L. H. Cohen, 2001: Bubble size distributions on the North Atlantic and the North Sea. *Gas Transfer at Water Surfaces,* M. A. Donelan et al., Eds., American Geophysical Union, 271–277.

——, M. M. Moerman, C. J. Zappa, W. R. McGillis, S. J. Norris, and M. H. Smith, 2007: Eddy correlation measurements of sea spray aerosol fluxes. *Transport at the Air–Sea Interface: Measurements, Models and Parameterizations,* C. S. Garbe, R. A. Handler, and B. Jähne, Eds., Springer-Verlag, 297–311.

Edson, J. B., A. A. Hinton, K. E. Prada, J. E. Hare, and C. W. Fairall, 1998: Direct covariance flux estimates from mobile platforms at sea. *J. Atmos. Oceanic Technol.,* **15,** 547–562.

Fairall, C. W., J. E. Hare, W. R. McGillis, J. B. Edson, and W. R. McGillis, 2000: Parameterization and micrometeorological measurements of air–sea gas transfer. *Bound.-Layer Meteor.,* **96,** 63–105.

Farmer, D. M., and Vagle, S., 1989: Waveguide propagation of ambient sound in the ocean-surface bubble layer. *J. Acoust. Soc. Amer.,* **86,** 1897–1908.

Frew, M. F., R. K. Nelson, W. R. McGillis, J. B. Edson, E. J. Bock, and T. Hara, 2002: Spatial variations in surface microlayer surfactants and their role in modulating air–sea exchange. *Gas Transfer at Water Surfaces, Geophys. Monogr.,* Vol. 127, Amer. Geophys. Union, 153–159.

Frew, N. M, and Coauthors, 2004: Air–sea gas transfer: Its dependence on wind stress, small-scale roughness, and surface films. *J. Geophys. Res.,* **109,** C08S17, doi:10.1029/2003JC002131.

Geever, M., C. D. O'Dowd, S. van Ekeren, R. Flanagan, E. D. Nilsson, G. de Leeuw, and Ü. Rannik, 2005: Submicron sea spray fluxes. *Geophys. Res. Lett.,* **32,** L15810, doi:10.1029/2005GL023081.

Graber, H. C., E. A. Terray, M. A. Donelan, W. M. Drennan, J. Van Leer, and D. B. Peters, 2000: ASIS—A new air–sea interaction spar buoy: Design and performance at sea. *J. Atmos. Oceanic Technol.,* **17,** 708–720.

Hardman-Mountford, N. J., and Coauthors, 2008: An operational monitoring system to provide indicators

of CO_2-related variables in the ocean. *ICES J. Mar. Sci.,* **65,** 1498–1503, doi:10.1093/icesjms/fsn110.

Hare, J. E., C. W. Fairall, W. R. McGillis, J. B. Edson, B. Ward, and R. Wanninkhof, 2004: Evaluation of the National Oceanic and Atmospheric Administration/ Coupled Ocean–Atmosphere Response Experiment (NOAA/COARE) air–sea gas transfer parameterization using GasEx data. *J. Geophys. Res.,* **109,** C08S11, doi:10.1029/2003JC001831.

Haywood J. M., V. Ramaswamy, and B. J. Soden. 1999: Tropospheric aerosol climate forcing in clear-sky satellite observations over the oceans. *Science,* **283,** 1299–1303.

Hill, M. K., B. J. Brooks, S. J. Norris, M. H. Smith, I. M. Brooks, and G. de Leeuw, 2008: A Compact Lightweight Aerosol Spectrometer Probe (CLASP). *J. Atmos. Oceanic. Technol.,* **25,** 1996–2006.

Ho, D. T., W. E. Asher, L. F. Bliven, P. Schlosser, and E. L. Gordan, 2000: On mechanisms of rain-induced air-water gas exchange, *J. Geophys. Res.,* **105,** 24 045–24 057.

Holliday, N. P., M. J. Yelland, R. W. Pascal, V. R. Swail, P. K. Taylor, C. R. Griffiths, and E. C. Kent, 2006: Were extreme waves in the Rockall Trough the largest ever recorded? *Geophys. Res. Lett.,* **33,** L05613, doi:10.1029/2005GL025238.

Huebert, B. J., B. W. Blomquist, J. E. Hare, C. W. Fairall, J. E. Johnson, and T. S. Bates, 2004: Measurement of the air–sea DMS flux and transfer velocity using eddy correlation. *Geophys. Res. Lett.,* **31,** L23113, doi:10.1029/2004GL021567.

Jähne, B., K. O. Münnich, R. Bosinger, A. Dutzi, W. Huber, and P. Libner, 1987: On the parameters influencing air–water gas exchange. *J. Geophys. Res.,* **92,** 1937–1949.

Johnson, B. D., and R. C. Cooke, 1979: Bubble populations and spectra in coastal waters: Photographic approach. *J. Geophys. Res.,* **84** (C7), 3761–3766.

Leifer, I., G. de Leeuw, and L. H. Cohen, 2003: Optical measurement of bubbles: System design and application. *J. Atmos. Oceanic Technol.,* **20,** 1317–1332.

Leighton, T. G., 2004: From seas to surgeries, from babbling brooks to baby scans: The acoustics of gas bubbles in liquids. *Int. J. Mod. Phys.,* **18B,** 3267–3314.

——, 2007: What is ultrasound? *Prog. Biophys. Mol. Biol.,* **93,** 3–83.

——, D. G. Ramble, and A. D. Phelps, 1997: The detection of tethered and rising bubbles using multiple acoustic techniques. *J. Acoust. Soc. Amer.,* **101,** 2626–2635.

——, A. D. Phelps, D. G. Ramble, and D. A. Sharpe, 1996: Comparison of the abilities of eight acoustic techniques to detect and size a single bubble. *Ultrasonics,* **34,** 661–667.

——, S. D. Meers, and P. R. White, 2004: Propagation through nonlinear time-dependent bubble clouds and the estimation of bubble populations from measured acoustic characteristics, *Proc. R. Soc. London, Ser. A,* **460,** 2521–5250.

Liss, P. S., and L. Merlivat, 1986: *The Role of Air–Sea Exchange in Geochemical Cycling.* P. Buat-Ménard, Ed., Series C: Mathematical and Physical Science, Vol. 185, Kluwer Academic, 113–129.

——, and Coauthors, 1997: Physical processes in the microlayer and the air–sea exchange of trace gases. *The Sea Surface and Global Change.* P. S. Liss and R. A. Duce, Eds., Cambridge University Press, 1–33.

——, and Coauthors, 2003: The SOLAS science plan and implementation strategy. International Geosphere–Biosphere Programme Rep. 50, 122 pp. [Available online at www.uea.ac.uk/env/solas/.]

Longuet-Higgins, M. S., and N. D. Smith, 1983: Measurement of breaking waves by a surface jump meter. *J. Geophys. Res.,* **88,** 9823–9831.

Mårtensson, M., E. D. Nilsson, G. de Leeuw, L. H. Cohen, and H.-C. Hansson, 2003: Laboratory simulations and parameterization of the primary marine aerosol production. *J. Geophys. Res.,* **108,** 4297, doi:10.1029/2002JD002263.

McGillis, W. R., J. B. Edson, J. E. Hare, and C. W. Fairall, 2001: Direct covariance air–sea CO_2 fluxes. *J. Geophys. Res.,* **106,** 16 729–16 745.

Monahan, E. C., and I. O'Muircheartaigh, 1980: Optimal power-law description of oceanic whitecap coverage dependence on wind speed. *J. Phys. Oceanogr.,* **10,** 2094–2099.

——, and ——, 1986: Whitecaps and the passive remote sensing of the ocean surface. *Int. J. Remote Sens.,* **7,** 627–642.

Nightingale, P. D., G. Malin, C. S. Law, A. J. Watson, P. S. Liss, M. I. Liddicoat, J. Boutin, and R. C. Upstill-Goddard, 2000: In situ evaluation of air–sea gas exchange parameterizations using novel conservative and volatile tracers. *Global Biogeochem. Cycles,* **14,** 373–387.

Nilsson, E. D., Ü. Rannik, E. Swietlicki, C. Leek, P. P. Aalto. J. Zhou, and M. Norma, 2001: Turbulent aerosol fluxes over the Arctic Ocean. 2. Wind-driven sources from the sea. *J. Geophys. Res.,* **106,** 32 139–32 154.

Norris, S. J., I. M. Brooks, G. de Leeuw, M. H. Smith, M. Moerman, and J. J. N. Lingard, 2008: Eddy covariance measurements of sea spray particles over the Atlantic Ocean. *Atmos. Chem. Phys.,* **8,** 555–563.

O'Dowd, C. D., and G. de Leeuw, 2007: Marine aerosol production: A review of the current knowledge.

Philos. Trans. Roy. Soc. London, **A365,** 1753–1774, doi:10.1098/rsta.2007.2043.

——, J. A. Lowe, and M. H. Smith, 1999: Coupling of sea-salt and sulphate interactions and its impact on cloud droplet concentration predictions. *Geophys. Res. Lett.,* **26,** 1311–1314.

Phelps, A. D., and T. G. Leighton, 1998: Oceanic bubble population measurements using a buoy-deployed combination frequency technique. *IEEE J. Oceanic Eng.,* **23,** 400–410.

——, D. G. Ramble, and T. G. Leighton, 1997: The use of a combination frequency technique to measure the surf zone bubble population. *J. Acoust. Soc. Amer.,* **101,** 1981–1989.

Pierrot, P. D., and Coauthors, 2009: Recommendations for autonomous underway pCO_2 measuring systems and data reduction routines. *Deep Sea Res. II,* doi:10.1016/j.dsr2.2008.12.005.

Stramska, M., and T. Petelski, 2003: Observations of oceanic whitecaps in the north polar waters of the Atlantic. *J. Geophys. Res.,* **108,** 3086, doi:10.1029/2002JC001321.

Tucker, M. J., and E. G. Pitt, 2001: *Waves in Ocean Engineering.* Ocean Engineering Book Series, Vol. 5, Elsevier, 521 pp.

Upstill-Goddard, R. C., A. J. Watson, J. Wood, and M. I. Liddicoat, 1991: Sulphur hexafluoride and helium-3 as seawater tracers: Deployment techniques and continuous underway analysis for sulphur hexafluoride. *Anal. Chim. Acta,* **249,** 555–562.

——, and Coauthors, 2007a: UK-SOLAS cruise report: RRS *Discovery* cruise D313, 07 November–06 December, 2006. DOGEE-SOLAS and SEASAW: High wind gas and aerosol fluxes in the North East Atlantic Ocean. British Oceanographic Data Centre, 109 pp. [Available online at www.bodc.ac.uk/data/information_and_inventories/cruise_inventory/report/d313.pdf.]

——, and Coauthors, 2007b: UK-SOLAS cruise report: RRS *Discovery* Cruise D320, 16 June–18 July, 2007. DOGEE-II: Air–sea gas exchange in the Atlantic Ocean. British Oceanographic Data Centre, 165 pp. [Available online at www.bodc.ac.uk/data/information_and_inventories/cruise_inventory/report/d320.pdf.]

Vagle, S., and D. M. Farmer, 1998: A comparison of four methods for bubble size and void fraction measurements. *IEEE J. Oceanic Eng.,* **23,** 211–222.

Wanninkhof, R., 1992: Relationship between wind speed and gas exchange over the ocean. *J. Geophys. Res.,* **97,** 7373–7382.

——, and W. R. McGillis, 1999: A cubic relationship between air–sea CO_2 exchange and windspeed. *Geophys. Res. Lett.,* **26,** 1889–1892.

——, K. F. Sullivan, and Z. Top, 2004: Air–sea gas transfer in the Southern Ocean. *J. Geophys. Res.,* **109,** C08S19, doi:10.1029/2003JC001767.

Watson, A. J., R. C. Upstill-Goddard, and P. S. Liss, 1991: Air–sea gas exchange in rough and stormy seas measured by a dual tracer technique. *Nature,* **349,** 145–147.

Woolf, D. K., 1997: Bubbles and their role in air–sea gas exchange. *The Sea Surface and Global Change,* P. S. Liss and R. A. Duce, Eds., Cambridge University Press, 173–205.

——, 2005: Parameterization of gas transfer velocities and sea-state-dependent wave breaking. *Tellus,* **57B,** 87–94.

Yelland, M. J., and R. W. Pascal, 2008: OWS *Polarfront* cruise P162i, 09 Sep–04 Oct 2006: HiWASE mobilization cruise. National Oceanography Centre Southampton Cruise Rep. 33, 40 pp.

——, B. I. Moat, P. K. Taylor, R. W. Pascal, J. Hutchings, and V. C. Cornell, 1998: Wind stress measurements from the open ocean corrected for air flow distortion by the ship. *J. Phys. Oceanogr.,* **28,** 1511–1526.

——, ——, R. W. Pascal, and D. I. Berry, 2002: CFD model estimates of the airflow distortion over research ships and the impact on momentum flux measurements. *J. Atmos. Oceanic Technol.,* **19,** 1477–1499.

——, K. Bjorheim, C. Gommenginger, R. W. Pascal, and B. I. Moat, cited 2007a: In-situ wave measurements at Station Mike. [Available online at waveworkshop.org/10thWaves/ProgramFrameset.htm.]

——, R. W. Pascal, P. K. Taylor, B. I. Moat, I. Skjelvan, and C. C. Neill, cited 2007b: High Wind Air–Sea Exchanges (HiWASE)—Continuous air–sea flux measurements at Station Mike. [Available online at http://ams.confex.com/ams/pdfpapers/125357.pdf.]

——, ——, ——, and ——, 2009: AutoFlux: An autonomous system for the direct measurement of the air–sea fluxes of CO_2, heat and momentum. *J. Oper. Oceanogr.,* **2** (1).

Zemmelink, H. J., W. W. C. Gieskes, P. M. Holland, and J. W. H. Dacey, 2002: Preservation of atmospheric dimethyl suphide samples on Tenax in sea-to-air flux measurements. *Atmos. Environ.,* **36,** 911–916.

——, L. Houghton, N. M. Frew, and J. W. H. Dacey, 2005: Gradients in dimethylsulfide, dimethylsulfoniopropionate, dimethylsulfoxide, and bacteria near the sea surface. *Mar. Ecol. Prog. Ser.,* **295,** 33–42.